8 Results and Discussion

8.1 PV Subsystem Results

Fig. 6 represents the controlled PV array output current against the reference maximum current. This is performed using different constant values of solar radiation. The maximum value of PV array current changes according to the solar radiation based on a linear relationship that exists between solar radiation and PV array output current. It is also clear from this figure that the system controller tracks the maximum current and so the PV array operates at maximum power point. For studying system behaviour under different circumstances over a complete day, variable radiation profiles are taken representing sunny day and cloudy day. Fig. 7 illustrates the PV output power versus maximum reference power for a sunny day, it is clear that the system tracks the maximum power point. The reference power values have been taken under standard climatological conditions. It also observed from curves that the shape of power curves is the same that of solar radiation curve as shown in Fig 8 which illustrates the incident solar radiation over the Kharga Oasis in W/m^2 starting from 0 at 5 AM and increasing as the sun rises until reaching a maximum value at 12 PM and decreasing again until sunset at 7 PM.

Simulation also was done using a radiation values for a cloudy day. Fig. 9 illustrates the PV array output power versus maximum power. It is observed from these figures that the solar radiation decreases and increases according to the existence of clouds and so the PV output power decreasing and increasing along the day taking the shape of solar radiation curve represented in Fig. 10. It can also be noted that the PI controller of the inverter tracks the maximum power point as the power curves of the PV output power and reference maximum power under these climatological conditions almost coincides.

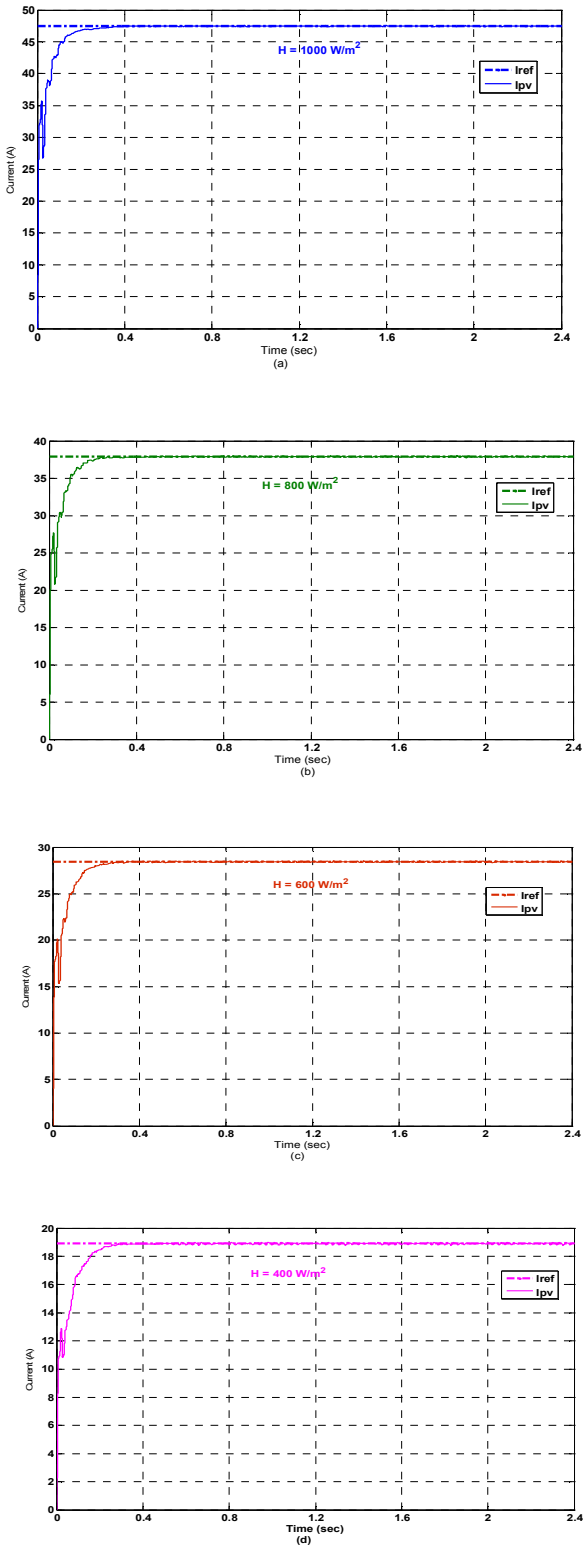

Fig. 6 The simulated PV array output currents for constant radiation values against reference maximum current.

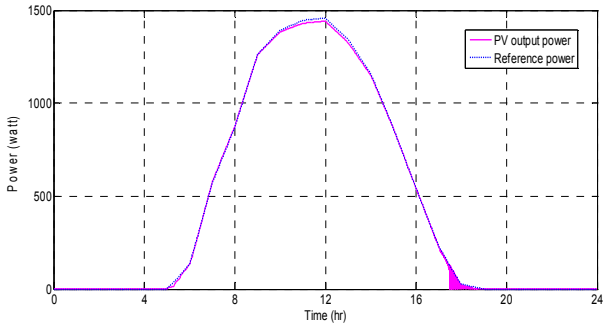

Fig. 7 Maximum PV output power and reference maximum power for a sunny day.

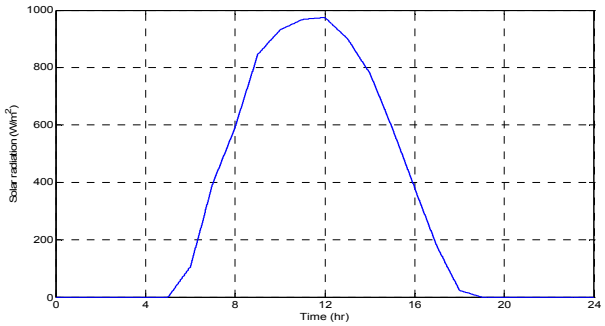

Fig. 8 The incident solar radiation over The Kharga Oasis in W/m^2 for a sunny day.

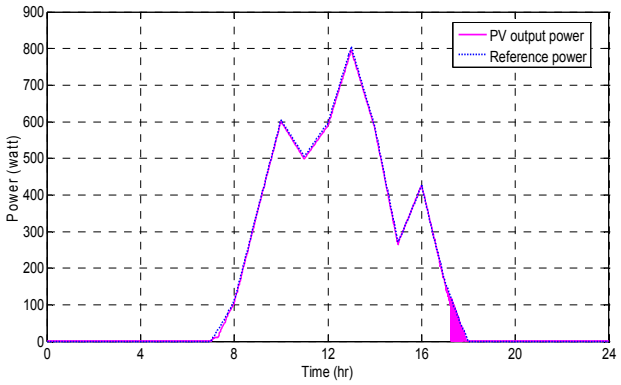

Fig. 9 Maximum PV output power and reference maximum power for a cloudy day.

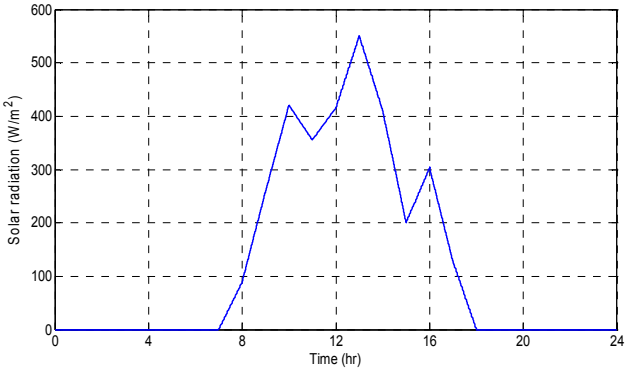

Fig. 10 The incident solar radiation over The Kharga Oasis in W/m^2 for a cloudy day.

8.2 Grid-Connected Mode Results

Fig. 11 shows the average power curves of the grid connected PV system for a sunny day. During night and early morning, the load is fed completely from the utility grid (S1 is off and S2 is on). At sunshine, the PV power becomes greater than 0 and the load is fed firstly from the PV array and the deficit power is supplied from the utility grid (S1 is on and S2 is on) while at peak sun hours from 7 AM to 8 AM and from 9 AM to 4 PM, the PV output power is greater than the load power and so the excess power is delivered to the electric grid. The average power curves of grid connected PV system for a cloudy day are illustrated in Fig. 12, the PV output power is low and the grid supply the deficit energy until 12 PM, so the power sold to the electric utility grid is lower than the power sold during sunny days.

The value of energy sold to the electric utility grid is 2.941 kWh/day for a sunny day and 0.42125 kWh/day for a cloudy day. Where, the energy purchased from the electric utility grid during cloudy days (10.74 kWh/day) is higher than the energy that purchased during sunny days (8.31 kWh/day) regarding that the load power consumption during summer is higher.

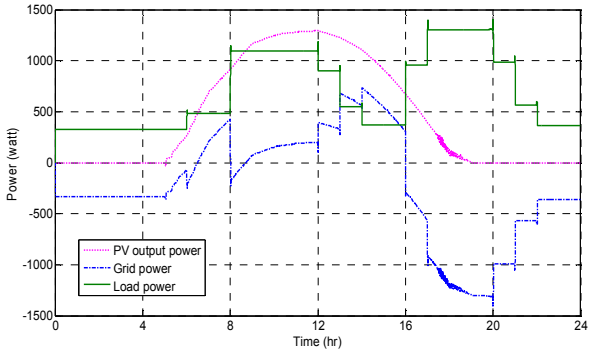

Fig. 11 Simulated generated power of PV, electric utility grid and load consumption for a sunny day.

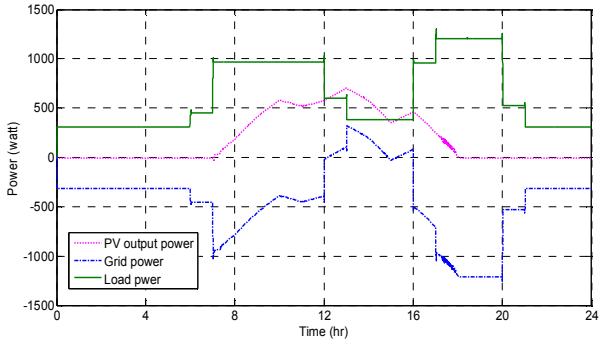

Fig. 12 Simulated generated power of PV, electric utility grid and load consumption for a cloudy day.

Fig. 13.a shows the current injected by the PV solar array after passing through power conditioning equipments (inverter, filter and transformer) with total harmonic distortion (THD) 0.81 %, the grid line current with THD of 1.08 % and the load current with THD 0.23%. The time interval of that figure is the early morning and sunshine period when the PV array starts to generate electrical power. The load is fed from utility grid, and then when the PV power exists, the load is fed from PV array and the deficit energy will be supplied from the utility grid. In the other hand, Fig. 13.b represents the current injected by the PV solar array, the grid line current and the load current during peak sun hour's period. It is observed that PV output current is higher than load current and so the surplus energy is being injected to the utility grid. During night, the PV output current is zero as shown in Fig. 13.c. It is also so clear that the load current and grid line current coincide which means that the load is fed completely from utility grid.

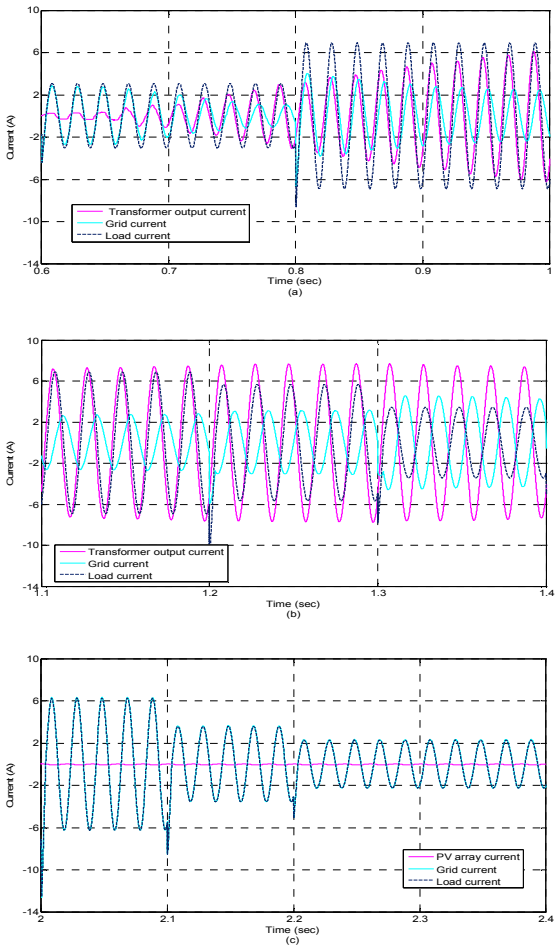

Fig. 13 Simulated transformer output current, grid current and load current.

8.3 Stand-Alone Mode Results

The stand alone mode contains the operation of the battery bank subsystem. The battery bank was designed to operate in parallel with the PV subsystem and feed the electrical loads of the clinic for a complete day in case of grid failure. Fig. 14 presents the battery power for a sunny day. As illustrated in the figure, in case of grid failure and during night and early morning hours, all load power demand is being discharged from the battery (S1 off, S2 off, S3 on and S4 off). Then, the PV output power increases but the load power increases and the power discharged from battery is the difference between the output PV power and load power (S1 on, S2 off, S3 on and S4 off). The discharged battery power then decreases as the PV power increases and when the PV array output power exceeds the load demand, this power is being delivered to the battery bank to be charged (S1 on, S2 off, S3 off and S4 on). In charging mode, the battery power is positive value from 7 AM up to 4 PM. After peak sun hours, the PV output power decreases and the deficit power is being discharged again from the battery bank.

Fig. 15 shows the battery power during a cloudy day, due to low generation the battery is heavily discharged to supply the deficit energy during day hours and completely fed the electrical loads during night. There is excess power only to the battery to be charged from 1 PM to 2 PM.

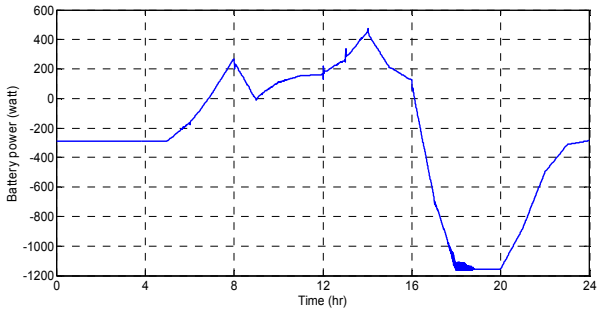

Fig. 14 Simulated battery power during a sunny day.

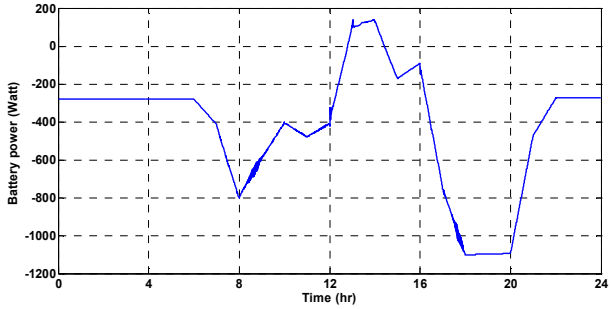

Fig. 15 Simulated battery power during a cloudy day.

The state of charge (SOC) of the battery is presented in Fig. 16 which gives an indication of the battery capacity level. It starts from 100% and then decreases as the battery at the discharging mode reaching a value of 92.5%. During charging, the SOC increases until 100% and decreasing again at discharging until reaching 75% at the end of the day. It is observed from SOC curve for a cloudy day as shown in Fig. 17 that the battery discharged to 57.7% at the end of the day and the excess power during day hours cannot charge the battery to its full capacity as sunny days due to low radiation levels in cloudy days and intermittent PV output power generation.

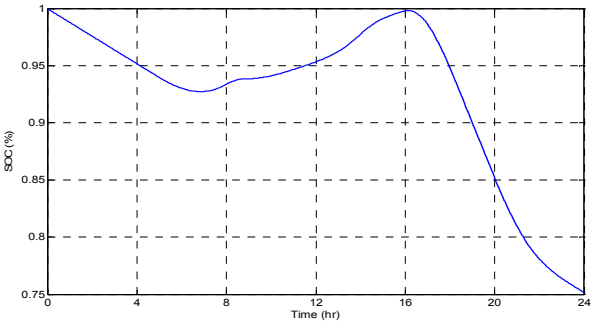

Fig. 16 Simulated SOC during a sunny day.

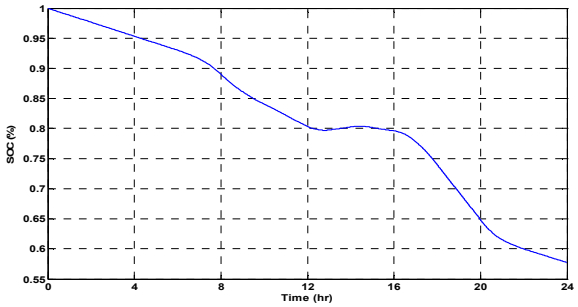

Fig. 17 Simulated SOC during a cloudy day.

8.4 Inverter results

The inverter works with a pulse width modulation technique. The IGBT switches are driven by a pulse generator controlled via PI controller which gives it the value of modulation index (m). Fig. 18 introduces the output pulse width modulation voltage of the inverter, which is represented by a square modulated AC wave. But it is shown that this signal contains high frequency switching harmonics, which can be eliminated by using low pass filter. The total harmonic distortion (THD) is very high reaching a value of about 67.38%.

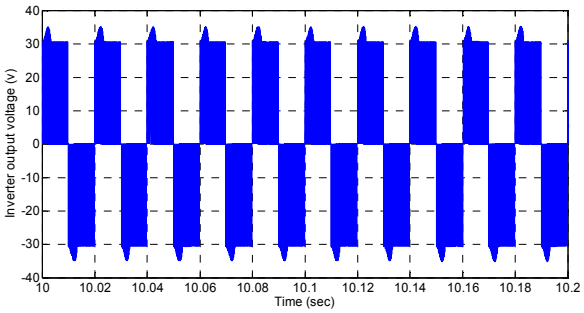

Fig. 18 Simulated PWM inverter output voltage.

8.5 Filter results

The cut off frequency of the filter is much higher than the signal fundamental frequency. The output voltage of filter is shown in Fig. 19 as pure sine wave with almost no harmonic contents and. The THD is 1.01% (below the world standard 3%) representing a very good signal to be delivered to the electrical grid and load.

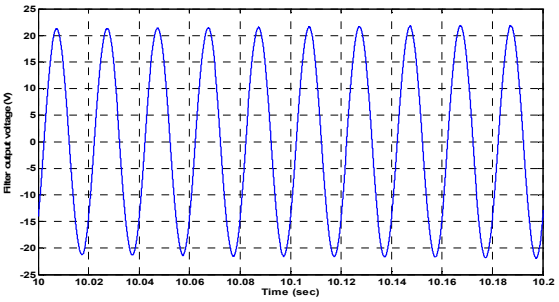

Fig. 19 The simulated filtered output voltage of the inverter.

8.6 Transformer Results

Transformer output voltage is shown in Fig. 20, it is clear that the transformer output voltage is almost pure sine wave of 220 VRMS value and 50 Hz fundamental frequency representing a very good signal consistent with the utility grid load requirements.

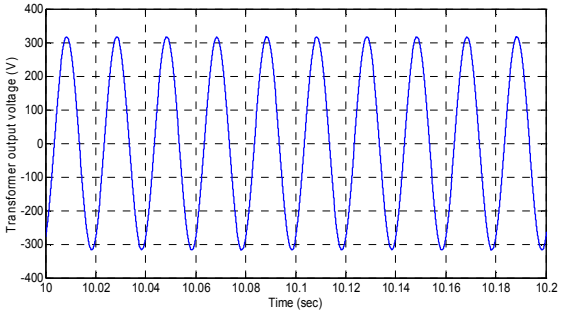

Fig. 20 Simulated transformer output voltage.

9 Conclusion

In this paper the mathematical model of all system components was introduced in order to investigate the dynamic behavior of each subsystem. Also the proposed control technique of the system was presented. This includes ON/OFF switch control of the system according to the modes of operation and inverter control using PI controller to track the maximum power point. The proposed system components models are implemented in Matlab/Simulink environment and interfaced with SimPowerSystem toolbox. The dynamic behavior of each subsystem is investigated showing the interaction between different components of grid connected PV system. The system gives a very good behavior for grid connected PV system mode and stand alone mode. The electrical loads of the clinic are completely supplied with electrical energy. The maximum power point is achieved. In case of stand alone mode and with the worst mode of operation (grid failure and cloudy day), the system gives good performance and the electrical loads are also completely supplied with electrical energy during the day. In that mode, the battery discharged until 57.7% above the discharging limit (30%) which means that there is a reserve capacity in the battery bank. The power conditioning units are well designed as the total harmonic distortion (THD) in the output voltage of the filter is 1.01% (below the world standard 3%) representing a very good signal to be delivered to the electrical grid and load. the current injected by the PV solar array after passing through power conditioning equipments (inverter, filter and transformer) has a THD of 0.81 %, the grid line current has a THD of 1.08% and the load current has a THD 0.23%.

References:

[1] Eftichios Koutroulis, Kostas Kalaitzaiis and Nicholas C. Voulgaris, Development of a microcontroller-based, photovoltaic maximum power point tracking control system, *IEEE Transactions on Power Electronics*, Vol. 16, No.1, Jan., 2001, pp. 46-54.

[2] Castaner Luis and Santiago Silvestre, *Modeling Photovoltaic systems using PSpice*, John Wiley and Sons Ltd, 2002.

[3] Arman Roshan, A dq rotating frame controller for single phase full-bridge inverters used in small distributed generation systems, *M.Sc. thesis*, Faculty of the Virginia Polytechnic Institute and State University, Jun., 2006.

[4] Dehbonei H., Borle L. and Nayar C.V., A review and a proposal for optimal harmonic mitigation in single-phase pulse width modulation, *Proceedings of 4th IEEE International Conference on Power Electronics and Drive Systems*, 2001, Vol. 1, Oct., 2001, pp. 408 – 414.

[5] Hossein Madadi Kojabadi, Bin Yu, Idris A. Gadoura, Liuchen Chang and Mohsen Ghribi, A Novel DSP-Based Current-Controlled PWM Strategy for Single Phase Grid Connected Inverters, *IEEE Transactions on Power Electronics*, Vol. 21, No. 4, Jul., 2006, pp. 98

[6] Khaled H. Ahmed, Stephen J. Finney and Barry W. Williams, Passive Filter Design for Three-Phase Inverter Interfacing in Distributed Generation, *Journal of Electrical Power Quality and Utilisation*, Vol. XIII, No. 2, 2007, pp. 49-58.

[7] E.Koutroulis, J.Chatzakis, K.Kalaitzakis and N.C.Voulgaris, A bidirectional, sinusoidal, high-frequency inverter Design, *IEE Proc.-Electr. Power Appl.*, Vol. 148, No. 4, Jul., 2001, pp. 315-321.

[8] V. Salas, E. Olı´as, A. Barrado and A. La´zaro, Review of the maximum power point tracking algorithms for stand-alone photovoltaic systems, *Solar Energy Materials & Solar Cells*, Vol. 90, 2006, pp. 1555–1578.

[9] S. Yuvarajan, Dachuan Yu and Shanguang Xub, A novel power converter for photovoltaic applications, *Journal of Power Sources*, Vol. 135, 2004, pp. 327–331.

[10] Trishan Esram, and Patrick L. Chapman, Comparison of Photovoltaic Array Maximum Power Point Tracking Techniques, *IEEE Transactions on Energy Conversion*, Vol. 22, No. 2, Jun., 2007, pp. 439-449.